



# Heat flux identification using reduced model and the adjoint method. Application to a brake disk rotating at variable velocity

S Carmona, Yassine Rouizi, O Quéméner, F Joly

## ► To cite this version:

S Carmona, Yassine Rouizi, O Quéméner, F Joly. Heat flux identification using reduced model and the adjoint method. Application to a brake disk rotating at variable velocity. The 7th International Conference on Computational Methods (ICCM2016), Aug 2016, Berkeley, United States. hal-02324443

**HAL Id: hal-02324443**

**<https://hal.science/hal-02324443>**

Submitted on 21 Oct 2019

**HAL** is a multi-disciplinary open access archive for the deposit and dissemination of scientific research documents, whether they are published or not. The documents may come from teaching and research institutions in France or abroad, or from public or private research centers.

L'archive ouverte pluridisciplinaire **HAL**, est destinée au dépôt et à la diffusion de documents scientifiques de niveau recherche, publiés ou non, émanant des établissements d'enseignement et de recherche français ou étrangers, des laboratoires publics ou privés.

# Heat flux identification using reduced model and the adjoint method. Application to a brake disk rotating at variable velocity

S. Carmona, Y. Rouizi, O. Quémener, F. Joly\*

Laboratoire de Mécanique et d'Energétique d'Evry, Université d'Evry Val d'Essonne  
40 rue du Pelvoux CE1455, Courcouronnes, 91020 Evry Cédex, France

\*Corresponding author : Frédéric JOLY (f.joly@iut.univ-evry.fr)

## Abstract

In previous works [1], reduced models have been used for solving inverse problems, characterized by a complex geometry requiring a large number of nodes and / or an objective of online identification. The treated application was a brake disc in two-dimensional representation, in rotation at variable speed. The dissipated heat flux at the pad-disk interface had been identified by Beck's method. We present here a similar application using the adjoint method. The modal reduction is done by using special bases (called branch bases) that offer the advantage of dealing with nonlinear problems and / or unsteady parameters. Adjoint method provides particularly accurate results in this configuration.

**Keywords** : Reduced model, Modal method, Inverse problem, Advection-diffusion equation, Adjoint method

## Nomenclature

$c$	Heat capacity [ $\text{J.m}^{-3}.\text{K}^{-1}$ ]
$e$	Disk thickness [m]
$k$	Thermal conductivity [ $\text{W.m}^{-1}.\text{K}^{-1}$ ]
$h$	Heat exchange coefficient [ $\text{W.m}^{-2}.\text{K}^{-1}$ ]
$U$	Disk velocity [ $\text{m.s}^{-1}$ ]
$T$	Temperature [ $^{\circ}\text{C}$ ]
$z_i$	Eigenvalue [ $\text{s}^{-1}$ ]
$x$	Modal temporal amplitude
$V$	Eigenvector [K]
$N_t$	Number of measurement steps

### *Greek symbols*

$\phi$	Heat flux [W]
$\omega$	Rotation velocity [ $\text{rad.s}^{-1}$ ]
$\zeta$	Steklov number [ $\text{kg.s}^{-2}.\text{K}^{-1}$ ]

### *subscript*

$u$	dimensionless quantity
$m$	Maximum Value
$\sim$	Reduced quantity
$\wedge$	Estimate

## Introduction

In the domain of heat conduction, inverse problems are generally ill-posed in the sense of Hadamard and then require complex procedures to obtain satisfactory results. Two techniques are used, the future time step method (Beck) [2] which has the particularity of being a sequential method, and the adjoint method [3] which is an iterative method based on successive computation of descent directions to minimize a criterion taking into account all the data.

In these inverse problems, mathematical complexity of the technique limits the size of the characteristic matrices of the thermal problem and the different studied geometries are often reduced to a simple, two-dimensional appearance. This problem is even more blatant when it comes to conduct an online identification, which involves fast calculations [4]. Under these conditions, the use of modal models [5], which allows a significant decrease in the number of unknowns while maintaining a satisfactory accuracy over the entire domain, allows the extension of the inverse techniques to geometries characterized by mesh of large size. Already developed to a diffusion-transport problem, this identification technique using low order

models involved the identification by Beck's method of the heat flux dissipated by friction during braking phases of a brake disk [1]. A similar configuration is studied in order to extend the use of reduced models to the adjoint method. A comparison between the two techniques is then presented.

### Position of the problem

A brake disk (Fig. 1) rotating at variable speed is considered. It receives during the braking phase a time dependant heat flux on the friction zone with the brake pads (domain  $\Omega_I$ ). In the studied case, the surrounding temperature is set to  $T_{ext} = 0^\circ\text{C}$  and the uniform initial temperature field is  $T_0 = 0^\circ\text{C}$ . The different time dependant parameters, the radial velocity  $\omega(t)$ , the heat exchange coefficient  $h(t)$  and flux dissipated by friction  $\phi(t)$  are expressed in terms of their maximum values and are therefore dimensionless:

$$\omega(t) = \omega_u(t) \omega_m, \quad (1)$$

$$h(t) = h_u(t) h_m, \quad (2)$$

$$\phi(t) = \phi_u(t) \phi_m = \phi_u(t) \int_{\Omega_I} \phi_m(r) d\Omega \quad (3)$$

The heat flux dissipated by friction  $\phi_m$  is not uniform on  $\Omega_I$  but varies linearly with velocity, so with the radius. The temporal evolution of  $\omega_u(t)$ ,  $h_u(t)$ , and  $\phi_u(t)$  are shown in Figure 2, and their maximum values are  $\omega_m = 2\pi \text{ rad/s}$ ,  $h_m = 110 \text{ W.m}^{-2}.\text{K}^{-1}$ , and  $\phi_m = 600 \text{ W}$ .

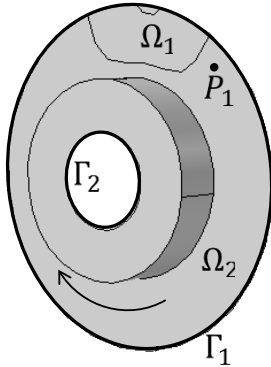


Figure 1 : Computational domain.

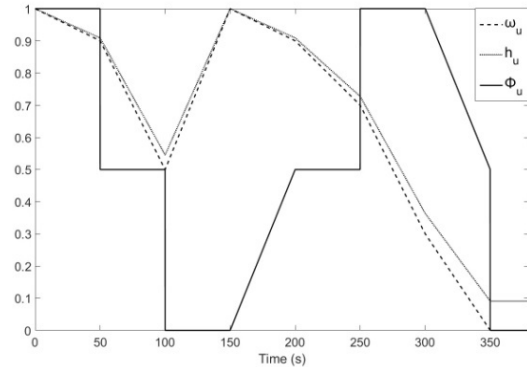


Figure 2 : Temporal evolution of thermal loads

### Numerical solution : the detailed model

Given the characteristic dimensions of the disk ( $k = 50 \text{ W.m}^{-1}.\text{K}^{-1}$ ,  $c = 3.66 \cdot 10^6 \text{ J.m}^{-3}.\text{K}^{-1}$ ,  $e = 8 \text{ mm}$ ), the Biot number corresponding to the worst case ( $h_m = 110 \text{ W.m}^{-2}.\text{K}^{-1}$ ) has a value  $\text{Bi} = 0.018 \ll 1$ . It is then possible to neglect the thermal gradient in the thickness  $e$  of the disc. By setting  $(\eta, \zeta)$  local coordinates  $\Omega$  in the plane perpendicular to this thickness, temperature is expressed as  $T(x, y, z) = T(\eta, \zeta)$ . This produces a thermal problem of shell type whose variational formulation is :

$$\begin{aligned} \int_{\Omega} e c \frac{\partial T}{\partial t} g d\Omega = & - \int_{\Omega} e k \bar{\nabla} T \cdot \bar{\nabla} g d\Omega - \omega_u(t) \int_{\Omega} e c \bar{U}_m \cdot \bar{\nabla} T g d\Omega \\ & - h_u(t) \left( \int_{\Omega_I} h_m T g d\Omega + \int_{\Gamma_I} h_m T g d\Gamma \right) + \phi_u(t) \int_{\Omega_2} \phi_m g d\Omega \end{aligned} \quad (4)$$

with  $g \in H_1(\Omega)$  a test function, and  $\Omega = \Omega_I \cup \Omega_2$ .

The discretization of this problem by linear finite element reveals a matrix system of dimension  $N$  (number of nodes) which is written in the order of previous terms:

$$\mathbf{C}\dot{\mathbf{T}} = [\mathbf{K} + \omega_u(t)\mathbf{U} + h_u(t)\mathbf{H}]\mathbf{T} + \phi_u(t)\mathbf{\Pi} \quad (5)$$

After a sensitivity analysis, the mesh consists of 9,860 nodes forming 19,362 triangle elements. For a direct problem, the temporal heat flux evolution is known and the evolution of the discrete temperature field  $\mathbf{T}$  is done by solving Eq. (5). Figure 3 represents the evolution of temperature at point A, placed 10mm downstream from the friction area (see Fig. 1). The analysis of the temperature field shows that the local friction on the  $\Omega_f$  area leads to the appearance of a sharp temperature front conveyed at the rotational speed. A fixed sensor detects a very rapid temperature variation, which as will be seen later makes the inverse problem difficult to solve.

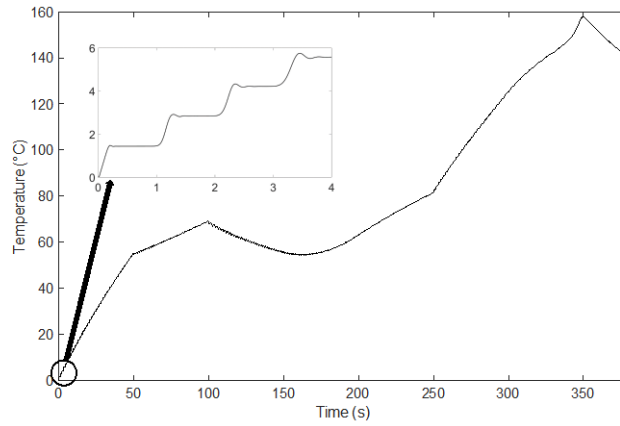


**Figure 3 :Temperature evolution at point A**

## Modal reduction

### *The branch problem*

The modal decomposition supposes the existence of a base such that the following decomposition is unique:

$$T(M, t) = \sum_{i=1}^N x_i(t) V_i(M) \quad (6)$$

where  $V_i(M)$  are eigenvectors (or modes), and  $x_i(t)$  are the unknown coefficients named hereafter modal amplitudes. The modes can be seen as elementary thermal fields.

The branch problem associates to the previous physical problem an eigenvalue problem defined by equations (7) and (8):

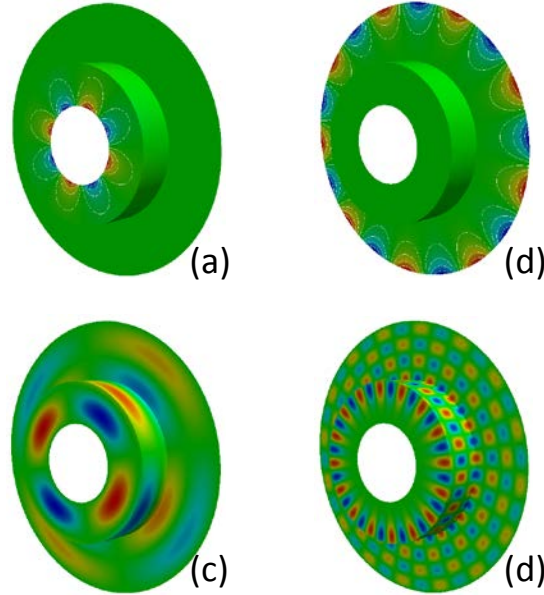
$$\forall M \in \Omega_1 \cup \Omega_2, \quad k \nabla^2 V_i = z_i c V_i \quad (7)$$

$$\forall M \in \Gamma_1 \cup \Gamma_2, \quad k \vec{\nabla} V_i \cdot \vec{n} = -z_i \zeta V_i \quad (8)$$

where  $z_i$  is the eigenvalue associated with the eigenvector  $V_i$ .

The boundary condition (Eq. (8)) is a non physical condition that involves the eigenvalue of the mode. The number of Steklov  $\zeta$  ensures dimensional homogeneity of the boundary condition and prevents degeneration of the modal problem, *i.e.* to balance Eqs. (7) and (8).

This special boundary condition reveals two types of modes. The first type is constituted of modes quasi null on the boundary but not on the domain (domain modes), and the second one formed of modes quasi null on the domain but not on the boundary (boundary modes). This second type of modes allows to link the temperature fields on the interface. Examples of such modes are given in Fig. 4. The existence of boundary modes allows one to rebuild temperature and thermal flux density for all convective coefficient. This basis is then adapted to nonstationary and nonlinear thermal problems.



**Figures 4 : Examples of branch modes : boundary modes ((a) and (b)) and domain modes ((c) and (d))**

#### *Reduction method*

The modal formulation only shifts the problem : instead of being temperature values at the nodes of a mesh, the unknowns are the amplitudes of the modes  $x_i(t)$ . The number of modes needed to approach correctly the solution needs to be reduced. This is done by the amalgam method [5] [6]. In this method, the most influential eigenmodes are kept (they are called major eigenmodes), and the remaining eigenmodes (called minor) are added to them, weighted by a factor  $\alpha_{i,p}$ . This results in new amalgamated eigenmodes  $\tilde{V}_i$ , which are a linear combination of eigenvectors of the original branch basis.

$$\tilde{V}_i = \sum_{p=0}^{n_i} \alpha_{i,p} V_{i,p} \quad (9)$$

The determination of factors  $\alpha_{i,p}$  is performed by minimizing the deviation of energy between a reference model and the reduced model. Note that in our case the reference problem used is constructed independently of the temporal evolution  $\phi_u(t)$  to be identified. With these amalgamated modes, the modal decomposition of temperature is given by :

$$T(M, t) \cong \sum_{i=1}^{\tilde{N}} \tilde{x}_i(t) \tilde{V}_i(M) \quad (10)$$

The amplitude equation is obtained by replacing the temperature by its modal decomposition (Eq. (10)) in the physical problem (Eq. (4)), while the test functions are the modes. It replaces

the problem on temperatures at the nodes of the mesh size by a problem on the temporal amplitudes of the modes. In discrete form, Eq. (4) becomes:

$$\begin{aligned} \mathbf{L}\dot{\tilde{\mathbf{X}}} &= [\mathbf{M}_{\mathbf{K}} + \omega_u(t)\mathbf{M}_{\mathbf{U}} + h_u(t)\mathbf{M}_{\mathbf{H}}] \tilde{\mathbf{X}} + \phi_u(t)\mathbf{N} \\ &= \mathbf{M}(t) \tilde{\mathbf{X}} + \phi_u(t)\mathbf{N} \end{aligned} \quad (11)$$

where  $\mathbf{L} = \tilde{\mathbf{V}}^t \mathbf{C} \tilde{\mathbf{V}}$ ,  $\mathbf{M}_{\mathbf{K}} = \tilde{\mathbf{V}}^t \mathbf{K} \tilde{\mathbf{V}}$ ,  $\mathbf{M}_{\mathbf{U}} = \tilde{\mathbf{V}}^t \mathbf{U} \tilde{\mathbf{V}}$ ,  $\mathbf{M}_{\mathbf{H}} = \tilde{\mathbf{V}}^t \mathbf{H} \tilde{\mathbf{V}}$  et  $\mathbf{N} = \tilde{\mathbf{V}}^t \mathbf{\Pi}$ ,  $\tilde{\mathbf{V}}$  being the matrix containing the  $\tilde{N}$  amalgamated eigenvectors, and vector  $\tilde{\mathbf{X}}$  contains the  $\tilde{N}$  temporal amplitude  $\tilde{x}(t)$ .

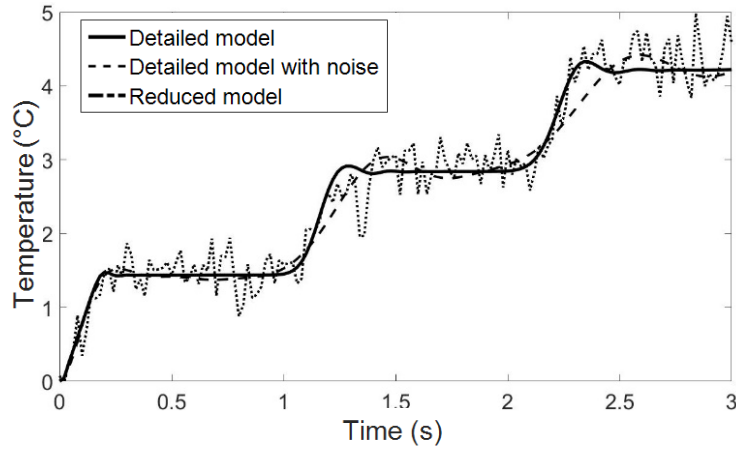


**Figure 5 :Temperature evolution at point A obtained with different models for the first 3 seconds of the simulation**

A reduced base with 50 modes is used. In the case of the direct problem (Eq. (11)), the modal model recovers the evolution of the thermal field with an average error compared to the detailed model of  $0.046^\circ\text{C}$  and a maximum error of  $6.18^\circ\text{C}$ , the temperature range being of  $139^\circ\text{C}$ , showing the good agreement between reduced and detailed models. At point A, the error averaged over time is  $0.105^\circ\text{C}$ . Figure 5 shows the temperature difference between these two models at the measurement point for the first seconds of the simulation.

### Inverse problem

The temporal evolution of the heat flux received by friction by the rotating disc is identified from an observable vector  $\mathbf{Y}$ , consisting here of a single measurement point located at A. Given the size of the discrete problem, modal formulation is used to reduce the size of the inverse problem. The relationship between the output vector  $\mathbf{Y}$  and the modal amplitude  $\mathbf{X}$  has to be added to the direct problem defined by equation (11) :

$$\mathbf{Y} = \mathbf{E}\mathbf{T} = \mathbf{E}\tilde{\mathbf{V}}\tilde{\mathbf{X}} \quad (12)$$

Two inversion techniques are used, Beck and adjoint method.

### Beck's method

Beck's method consists in determining the amplitude of flux at each time step so that the temperature difference between the measurement and the simulation is the smallest possible.

An implicit time discretization (at a fixed time-step  $\Delta t = 0.02$  s) of Eq. (11) yields the amplitude of each mode:

$$\tilde{\mathbf{X}}^{k+1} = [\mathbf{L} - \Delta t \mathbf{M}(t)]^{-1} [\mathbf{L} \tilde{\mathbf{X}}^k + \Delta t \phi_u^{k+1} \mathbf{\Pi}] \quad (13)$$

A least squares minimization between measurement and temperature computed from the estimate at the previous time-step brings the estimation of the searched solicitation :

$$\phi_u = [\mathbf{\Theta}^t \mathbf{\Theta}]^{-1} \mathbf{\Theta}^t \mathbf{Z}^{k+1} \quad (14)$$

with  $\mathbf{\Theta}$  and  $\mathbf{Z}$  defined by :

$$\mathbf{\Theta} = \mathbf{E}[\mathbf{L} - \Delta t \mathbf{M}]^{-1} [\Delta t \mathbf{\Pi}] \quad (15)$$

$$\mathbf{Z}^{k+1} = \mathbf{Y}^{k+1} - \mathbf{E}[\mathbf{L} - \Delta t \mathbf{M}]^{-1} [\mathbf{L} \hat{\mathbf{X}}^k] \quad (16)$$

This technique is first used in an ideal case, wherein the temperature variation at point A used for identification comes directly from the simulation performed by the reduced model. There is then no error in this situation between the measurement and the direct model. The accuracy of the identification carried out is characterized by global error on the flux ( $\sigma_{\phi_u}$ ) and the temperature ( $\sigma_T$ ), which are defined by equations (17) and (18)

$$\sigma_T = \sqrt{\frac{\sum_{i=1}^{i=Nt} (Y(i) - \hat{Y}(i))^2}{Nt}} \quad (17)$$

$$\sigma_{\phi_u} = \sqrt{\frac{\sum_{i=1}^{i=Nt} (\phi_u(i) - \hat{\phi}_u(i))^2}{Nt}} \quad (18)$$

These simulations were performed for a time-step equal to 0.02s. The choice of this reduced time-step is explained by the influence of the transport term that creates sudden temperature changes that need to be taken into account for identification. The choice of the time-step then does not depend on the simple diffusion time between the source and the sensor, but also on the time of transport and the ability of the model to detect sudden changes in temperature. In an ideal case, results are satisfying as  $\sigma_{\phi_u} = 0.039$  and  $\sigma_T = 0.962^\circ\text{C}$ .

In a real case, the temperature of a probe is simulated by the full thermal model (Eq. (5)), to which is added a Gaussian white noise characterized by a quadratic error  $\sigma_b = 0.3^\circ\text{C}$ . In this case the identification results are directly unusable: the error on the identified flux is  $\sigma_{\phi_u} = 1.59$ . Indeed, as shown in Fig. 5, the bias to both the use of reduced model in the inverse procedure and measurement error strongly modifies the rapid changes in temperature. The various regularization attempts (increasing the number of measurement points, using a growing number of future time-steps) do not improve significantly the results. This problem had already been shown in previous work [1], and the recommended solution was the use of a low-frequency filter on the identified flux by Fourier transform, assuming that any variation

frequency greater than the frequency rotation could only be a numerical distortion. The application of this technique to our configuration is shown in Figure 6. The results are satisfactory since the use of a 0.4 Hz cutoff frequency results in an error on the identified flow equal to  $\sigma_{\phi_u} = 0.038$  and an error on the temperature  $\sigma_T = 0.832$  °C.

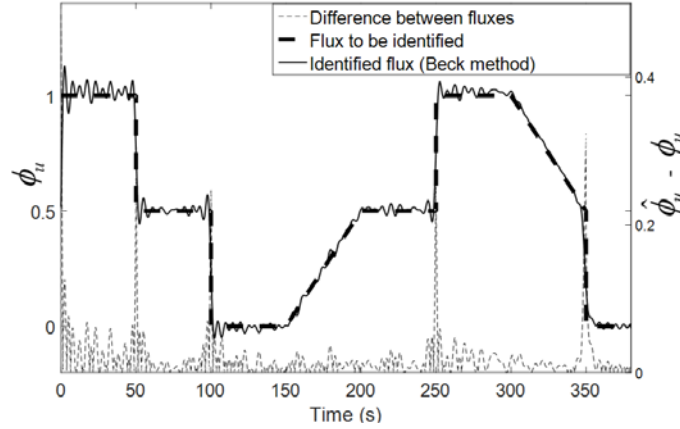


**Figure 6 :Heat flux identification obtained with Beck's method after filtering**

#### *Adjoint method*

The second inversion technique is the adjoint method. It is a global method in which a quadratic functional built on the differences between the measured temperatures and those computed with the identified heat flux is minimized. This function can also be penalized by a regularization term  $\varepsilon$  :

$$J(\phi_u) = \frac{1}{2} \left[ \int_0^{\tau} \|\mathbf{Y}(t) - \hat{\mathbf{Y}}(t)\|^2 dt + \varepsilon \|\phi_u(t)\|^2 \right] \quad (19)$$

The identification process consists in finding optimum solicitations  $\bar{\phi}_u$  such that J is minimum.

$$\bar{\phi}_u = \arg[\min J(\phi_u)] \quad (20)$$

This problem is solved using a descent method. These methods require the estimation of the functional gradient with respect to the solicitations. The amplitude equation of the model can be seen as a constraint between the thermal loads and temperatures. It involves the Lagrangian  $L_a$  associated with the minimization problem under the constraint of the state equation. This term is constructed by summing the functional and the state equation weighted by a Lagrange multiplier ( $\lambda$ ):

$$L_a(\phi_u, T, \lambda) = J(\phi_u) + \int_0^{\tau} \lambda(t) \left( -\mathbf{L} \frac{d\tilde{\mathbf{X}}}{dt} + \mathbf{M}\tilde{\mathbf{X}} + \mathbf{N}\phi_u \right) dt \quad (21)$$

At the point where the functional is minimal, the derivatives of the Lagrangian with respect to these three variables are null :

$$\frac{\partial L_a}{\partial \lambda} = 0 \quad (22)$$

$$\frac{\partial L_a}{\partial \phi_u} = 0 \quad (23)$$

$$\frac{\partial L_a}{\partial T} = 0 \quad (24)$$



The computation of derivative defined by Eq. (22) retrieves the amplitude equation (Eq. (11)). The two last derivatives (Eqs. (23) and (24)) bring two new relations, called gradient equation and adjoint equation:

$$\nabla \mathbf{J} = \varepsilon \mathbf{U} - \mathbf{\Pi}^t \mathbf{V} \boldsymbol{\lambda} \quad (25)$$

$$-\mathbf{L} \dot{\boldsymbol{\lambda}} = \mathbf{M}^* \boldsymbol{\lambda} + \mathbf{V}^t \mathbf{E}(\mathbf{Y}(t) - \hat{\mathbf{Y}}(t)) \quad (26)$$

where  $\mathbf{M}^*$  is the adjoint matrix of  $\mathbf{M}$ .

Thus the interest of this formulation is to compute the gradient  $\nabla \mathbf{J}$  (Eq. (25)) from the resolution of the single equation (26). The iterative calculation of the thermal load  $\phi_u^k$  is done using this gradient  $\nabla \mathbf{J}$ . Many descent patterns exist. We present here the conjugate gradient method, which combines the flux value at a previous iteration with a descent direction (noted  $\mathbf{w}^k$  here):

$$\phi_u^{k+1} = \phi_u^k + \rho^k \mathbf{w}^k \quad (27)$$

This iterative calculation is finished when one of the following criteria is met. The first is based on the evolution of the functional  $J$  (Eq. (28)). The second compares the difference between the estimated temperature and the measurements, which should be of the same order of magnitude as the level of uncertainty of the measurement (principle of Morozov Eq. (29)).

$$\frac{J(\phi_u^k) - J(\phi_u^{k-50})}{J(\phi_u^k)} < 1\% \quad (28)$$

$$\sigma_T \approx \sigma_b \quad (29)$$

The direction of descent  $\mathbf{w}^k$  is a combination between the current and previous descent directions weighted by a coefficient  $\gamma^k$  called Fletcher-Reeves conjugation parameter:

$$\mathbf{w}^k = \gamma^k \mathbf{w}^{k-1} - \nabla \mathbf{J}^k \quad (30)$$

$$\gamma^k = \frac{\|\nabla \mathbf{J}^k\|^2}{\|\nabla \mathbf{J}^{k-1}\|^2} \quad (31)$$

and  $\rho^k$  is the optimal descent step, computed by the secant method ( $\alpha$  is a small non null random number)

$$\rho^k = -\alpha \frac{\langle \nabla \mathbf{J}(\phi_u^k), \mathbf{w}^k \rangle}{\langle \nabla \mathbf{J}(\phi_u^k + \alpha \mathbf{w}^k), \mathbf{w}^k \rangle - \langle \nabla \mathbf{J}(\phi_u^k), \mathbf{w}^k \rangle} \quad (32)$$

The treated case corresponds to noisy temperatures ( $\sigma_b = 0.3$  °C) issued from the detailed model. In the inverse procedure, the penalization term is null ( $\varepsilon = 0$ ). The above presented algorithm converges to the imposed flux in 379 iterations. As shown in Figure 7, this method does not need additional filtering to recover properly the temporal flux variations. Flux deviation is  $\sigma_{\phi_u} = 0.051$ , which is very slightly greater than the deviations obtained by Beck's method with low frequency filtering, and in terms of temperatures  $\sigma_T = 0.389$  °C, which is less than the error obtained by Beck's method with filtering.

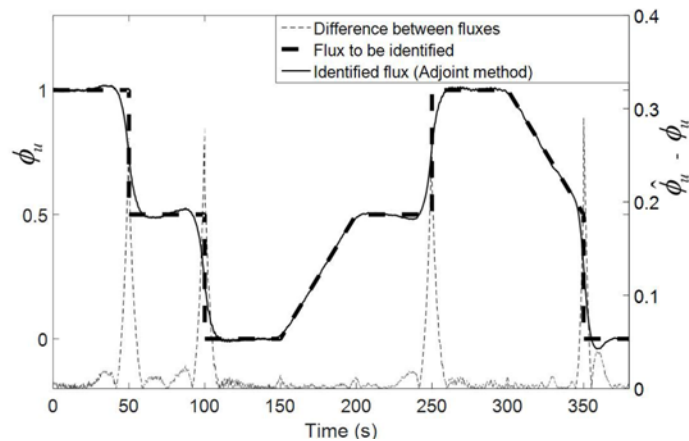


**Figure 7 : Heat flux identification with adjoint method**

Obtaining such satisfying results without filtering can be explained by the fact that the estimated flux is issued from a minimization including the entire temperature variation. In contrast, in Beck's method only the next time step is used to estimate the flux at a given time, which makes this technique much more sensitive to sudden changes and noise measurements.

## Conclusion

The study first of all showed the interest of using low order models in inverse problems, as the loss of information generated by the reduction remains below the noise measurements. Regarding the comparison of the two inverse techniques used in this paper, results showed the difficulty in obtaining correct results with Beck's method. In fact, the sequential aspect of this method does not filter the errors directly obtained from the measurement which are amplified significantly during the flux identification process. A solution is possible, however, but at the cost of additional low frequency filtering, which eliminates the sequential aspect of this technique. The effectiveness of the adjoint method was shown, since very satisfactory results were obtained, with no obligation to use any additional filtering or penalty term functional. This method, more comprehensive, naturally filters the noise during the functional minimization process. The price to pay is that the adjoint method requires more computation time (750s) than Beck's method (115s). These are very encouraging results, paving the way for online identification, both by a search for the minimum acceptable reduction of the modal model, and by the development of a more appropriate adjoint technique (order 2 descent method, temporal sliding window).

## Références

- [1] O. Quémener, F. Joly, A. Neveu (2009), On-line heat flux identification from a rotating disk at variable speed, *Int. J. of Heat and Mass Transfer* 53, 1529-1541
- [2] S. Chantasiriwan (2001), An algorithm for solving multidimensional inverse heat conduction problem, *Int. J. of Heat and Mass Transfer* 44, 3823-3832
- [3] R.A. Khachfe, Y. Jarny (2001), Determination of heat sources and heat transfer coefficient for two-dimensional heat flow - numerical and experimental study. *Int. J. of Heat and Mass Transfer* 1309-1322
- [4] A. Vergnaud, L. Perez, L. Autrique (2016), Quasi-online parametric identification of moving heating devices in a 2D geometry, *Int. J. of Thermal Sciences*, 102, 47-61
- [5] O. Quémener, A. Neveu, E. Videcoq (2006), A specific reduction method for branch modal formulation : Application to highly non linear configuration, *Int. J. of Thermal Sciences* 46, 890-907.
- [6] O. Quémener, F. Joly, and A. Neveu (2012), The generalized amalgam method for modal reduction, *Int. J. Heat and Mass Transfer*, 55, 1197-1207